

# Turbulence Descriptors for Scaling Fatigue Loading Spectra of Wind Turbine Structural Components

N. D. Kelley  
*Prepared for the  
IEA Expert Meeting on "Wind Conditions  
for Wind Turbine Design"  
June 27-28, 1994  
Hamburg, Germany*



National Renewable Energy Laboratory  
1617 Cole Boulevard  
Golden, Colorado 80401-3393  
A national laboratory of the U.S. Department of Energy  
Managed by Midwest Research Institute  
for the U.S. Department of Energy  
under contract No. DE-AC36-83CH10093

Prepared under Task No. WE418010

July 1994

### **NOTICE**

**NOTICE:** This report was prepared as an account of work sponsored by an agency of the United States government. Neither the United States government nor any agency thereof, nor any of their employees, makes any warranty, express or implied, or assumes any legal liability or responsibility for the accuracy, completeness, or usefulness of any information, apparatus, product, or process disclosed, or represents that its use would not infringe privately owned rights. Reference herein to any specific commercial product, process, or service by trade name, trademark, manufacturer, or otherwise does not necessarily constitute or imply its endorsement, recommendation, or favoring by the United States government or any agency thereof. The views and opinions of authors expressed herein do not necessarily state or reflect those of the United States government or any agency thereof.

Printed in the United States of America

Available to DOE and DOE contractors from:

Office of Scientific and Technical Information (OSTI)

P.O. Box 62

Oak Ridge, TN 37831

Prices available by calling (615) 576-8401

Available to the public from:

National Technical Information Services (NTIS)

U.S. Department of Commerce

5285 Port Royal Road

Springfield, VA 22161

(703) 487-4650



IEA Annex IX  
Expert Meeting, *Wind Conditions for Wind Turbine Design*  
Hamburg, June 27-28, 1994

## **TURBULENCE DESCRIPTORS FOR SCALING FATIGUE LOADING SPECTRA OF WIND TURBINE STRUCTURAL COMPONENTS**

**N.D. Kelley**  
**Wind Technology Division**  
**National Renewable Energy Laboratory**  
**Golden, Colorado U.S.A.**

### **Introduction**

The challenge for the designer in developing a new wind turbine is to incorporate sufficient strength in its components to *safely* achieve a 20- or 30-year service life. To accomplish this, the designer must understand the load and stress distributions (in a statistical sense at least) that the turbine is likely to encounter during its operating life. Sources of loads found in the normal operating environment include start/stop cycles, emergency shutdowns, the turbulence environment associated with the specific site and turbine location, and extreme or "rare" events that can challenge the turbine short-term survivability. Extreme events can result from an operational problem (e.g., controller failure) or violent atmospheric phenomena (tornadic circulations, strong gust fronts). For the majority of the operating time, however, the character of the turbulent inflow is the dominant source of the alternating stress distributions experienced by the structural components. Methods of characterizing or scaling the severity of the loading spectra (or the rate of fatigue damage accumulation) must be applicable to a wide range of turbulent inflow environments— from solitary isolation to the complex flows associated with multi-row wind farms. The metrics chosen must be related to the properties of the turbulent inflow and independent of the nature of local terrain features.

### **Scaling of Loading Spectra by Turbulence Descriptors**

The stochastic characteristics of the turbulent inflow are the major significance in influence on the rate accumulation of alternating (range or peak-to-peak) stress cycles experienced by structural components in wind turbines. Recently we showed that the distributions of these cycles can be described by a mixture of at least three parametric statistical models [1-3]. The contribution of each of the component distributions is diagrammed in Figure 1. Recent analyses of the loading events associated with turbine rotor blades have shown that the majority of the fatigue damage is associated with events occurring relatively infrequently, as compared with the turbine rotation rate (low-cycle), but with high amplitudes. We will subsequently refer to this range as the low-cycle, high-amplitude (*LCHA*) range. We found that, except for the in-plane or edgewise blade bending, the LCHA range is described by a decaying exponential distribution. An extreme value (Type I) distribution appears to describe the edgewise bending loads whose shape is strongly influenced by the once-per-revolution gravity load.

In another analysis, we compared several statistical descriptors of the turbulent inflow with the shape parameters of the decaying exponential distribution of the root flapwise loading and the extreme value

distribution of the root edgewise loads in the LCHA range [4]. The data from an extensive series of measurements of the simultaneous operation of two adjacent Micon 65/13 turbines deep within a large wind farm in the San Geronio Pass, California. We found that the upper (high) frequency bound of the LCHA range could be described as 100 cycles/hour. We believe that the asymptotic behavior observed in *the LCHA load range* is a consequence of the cycle-counting process being *Markov-Poisson*. This means that, for record lengths or counting periods where stationarity can be assumed, the events (the closing of hysteresis stress/strain cycles) are independent of one another and their number depends only on the record length. For the highly unsteady conditions present in a wind farm environment, quasi-stationarity can only be assumed to exist for periods near 10 minutes. Because the turbulence in the turbine inflow is the ultimate excitation of the observed load cycles, we suggest that the process can be described as *non- or inhomogeneous* Markov-Poisson whose scaling varies with time.

We determined the sensitivity of the distribution shape parameters to inflow fluid dynamics parameters by classifying the observed population of 10-minute records with respect to atmospheric stability and mean hub-height horizontal wind speed. A number of turbulence descriptors measured at hub height were calculated for each of the classes: mean horizontal wind speed and standard deviation, turbulence intensity, medians of the components of the mean shear (Reynolds) stresses, and gradient Richardson number stability criteria. By cross-correlating these bulk measures with the distribution shape parameters, we determined that they were most sensitive to the stability and the hub-height mean shear stress  $u'w'$  ( $u_*$ ). Figures 2 and 3 summarize these correlations for the flap and edgewise bending loads, respectively. We also found a narrow range of slightly stable flow conditions in which the exponential distribution slope reaches its minimum and the extreme value distribution (edgewise bending) reaches its maximum. Such conditions indicate a *broad range* of load cycles are present. This stability range was also found to contain the highest values of the cross-covariances for the three wind components, indicating that the flow was dominated by highly correlated or coherent structures. As shown in Figure 4, the majority of the 25 largest flapwise bending loads in the Micon 65 data set were in this stability range.

### **Damaging Loads and Coherent Turbulent Structures**

We believe the conditions present in this narrow stability range support the existence of dynamic instability in the internal wind-farm flows. Under these conditions, small-scale perturbations such as those making up turbine wakes can grow exponentially with time. Also, within the layer containing the turbine rotors, this range of stability can support the development of internal gravity waves and transient shear-generated phenomena such as Kelvin-Helmholtz instabilities. At this point we are unsure about the size of the disturbances (relative to the dimensions of the rotor) responsible for the largest peak loads observed on the turbine rotors. We do know, however, that these disturbances move vertically as well as horizontally through the disks. Figure 5 demonstrates the character of large flapwise loads encountered in two stability regimes. Case A took place in a less-stable flow where the stability parameter  $z/L$  was +0.007 as compared with Case B where it was +0.041.

During the year prior to making the measurements on the Micon turbines, we measured extensively the turbulence characteristics from two 50-m towers installed at two other locations in this large 41-row wind farm. One tower was placed immediately upwind of the first row of the farm and the other immediately downstream. We collected more than 4 weeks of data with both towers in simultaneous, 24-hour operation during the peak of the San Geronio wind season. From these results, we developed site-specific turbulence models for both environments [5]. We later included in the modeling the data collected in conjunction with the following year's Micon measurements. The results allow us to examine statistically the diurnal conditions in which the presence of coherent turbulent structures is indicated, and

therefore, the possibility of increased damaging loads in the exposed turbines. Figure 6 summarizes the measurements of  $u'w'$ , as a function of the hub-height mean wind speed and 5-to-50 meter layer stability expressed as the  $z/L$  parameter. A noticeable difference exists between turbulence environments upwind (Row 1) and within or downstream of the farm. The Micon test turbines were located at Row 37 and the downstream tower beyond Row 41; the former had an operating row of turbines immediately upstream for a spacing of seven turbine rotor diameters (7D), whereas the nearest operating turbine upstream of the downwind tower was two rows or 14D. The rate of mean shear stress increase with increasing wind speed is much greater within and downstream of the farm, reflecting the impact of the turbine wakes and the strong shear zone immediately above the turbines. The effect of the 7D spacing is seen in the higher mean shear stress and its high rate of increase with wind speed. Further, the levels remain elevated with increasing stability, in comparison with the upwind and downwind tower locations.

### Modeling the LCHA Loading with Coherent Turbulent Events

We have used the site-specific turbulence models to generate a range of simulated inflows to drive turbine dynamic simulations based on the ADAMS® (Automatic Dynamic Analysis of Mechanical Systems) multi-body simulation code. We recently simulated four turbulence inputs based on hub-height wind speeds of 12 and 17  $\text{ms}^{-1}$  and two spectral models. Two of the simulated inflows are based on the IEC TC-88 Kaimal spectral model. The remainder are based on conditions seen at Row 37 (7D spacing) when frequent activity in the LCHA load range has been noted. The turbine simulated was a downwind machine with a two-bladed rotor and teetered hub [6]. The flap and edgewise alternating blade loading (range) spectra for the four simulated turbulence cases are summarized in Figure 7. Table 1 summarizes a number of turbulence statistical parameters calculated from the hub station for the four turbulence simulations. The relationship between the simulated wind farm environments and the observed mean stress distributions for three wind farm stations are shown in Figures 8, 9, and 10. The impact of encountering a coherent turbulent structure on the teeter angle and flap- and edgewise blade root loads is presented in Figure 11.

**Table 1. Measured Turbulence Descriptors for Simulated Turbulent Flows at Hub Height.**

Spectral Model	$U_H$ ( $\text{ms}^{-1}$ )	$(u'w')^{1/2}$ ( $\text{ms}^{-1}$ )	$(u'v')^{1/2}$ ( $\text{ms}^{-1}$ )	$(v'w')^{1/2}$ ( $\text{ms}^{-1}$ )	$\sigma_H$ ( $\text{ms}^{-1}$ )	$z/L$	Power Law Coefficient
IEC-TC88K	12	-0.172	0.146	0.103	1.90	0	0.200
San Gor 7D	12	-1.494	-0.843	0.679	2.59	+0.005	0.123
IEC-TC88K	17	-0.223	0.203	0.139	2.64	0	0.200
San Gor 7D	17	-1.880	-0.953	0.851	3.29	+0.005	0.123

## Conclusions

We have presented evidence that the fatigue loads in the low-cycle (100 cycles per hour or less), high-amplitude range are influenced by the degree of coherency in the turbulence inflow. By applying an appropriate statistical distribution to this range, the distribution shape parameters can be scaled by knowing the mean hub-height shearing stress and stability of the inflow. The higher shear stresses are associated with increased activity in the LCHA and further increases are noted within a wind farm when slightly stable flows are present. These results indicate that damaging turbine loads scale with more than just the mean wind speed and turbulence intensity. In the design of wind turbines, a more conservative position is necessary in defining the lifetime loading distributions if the turbines are to be used in multi-row wind farms.

## Acknowledgments

This work has been supported by the U.S. Department of Energy under contract number DE-AC02-83CH10093.

## References

1. Kelley, N., Desrochers, G., Tangler, J., and Smith, B., October 1992, "A Discussion of the Results of the Rainflow Counting of a Wide Range of Dynamics Associated with the Simultaneous Operation of Adjacent Wind Turbines," NREL/TP-442-5159, National Renewable Energy Laboratory, Golden, CO.
2. Kelley, N.D., June 1993, "Defining the Normal Turbine Inflow Within a Wind Park Environment," NREL/TP-442-5619, National Renewable Energy Laboratory, Golden, CO.
3. Kelley, N.D., July 1993, "Inflow Characteristics Associated with High-Blade-Loading Events in a Wind Farm," NREL/TP-442-5623, National Renewable Energy Laboratory, Golden, CO.
4. Kelley, N.D., November 1992, "Full Vector (3-D) Inflow Simulation in Natural and Wind Farm Environments Using an Expanded Version of the SNLWIND (Veers) Turbulence Code," NREL-TP-442-5225, National Renewable Energy Laboratory, Golden, CO.
5. Kelley, N.D., January 1994, "The Identification of Inflow Fluid Dynamics Parameters That Can Be Used to Scale Fatigue Loading Spectra of Wind Turbine Structural Components," NREL-TP-442-6008, National Renewable Energy Laboratory, Golden, CO.
6. Malcolm, D. J. and Wright, A. D., January, 1994, "The Use of ADAMS to Model the AWT-26 Prototype," In Proceedings of Wind Energy 1994, American Society of Mechanical Engineers, New York, NY.

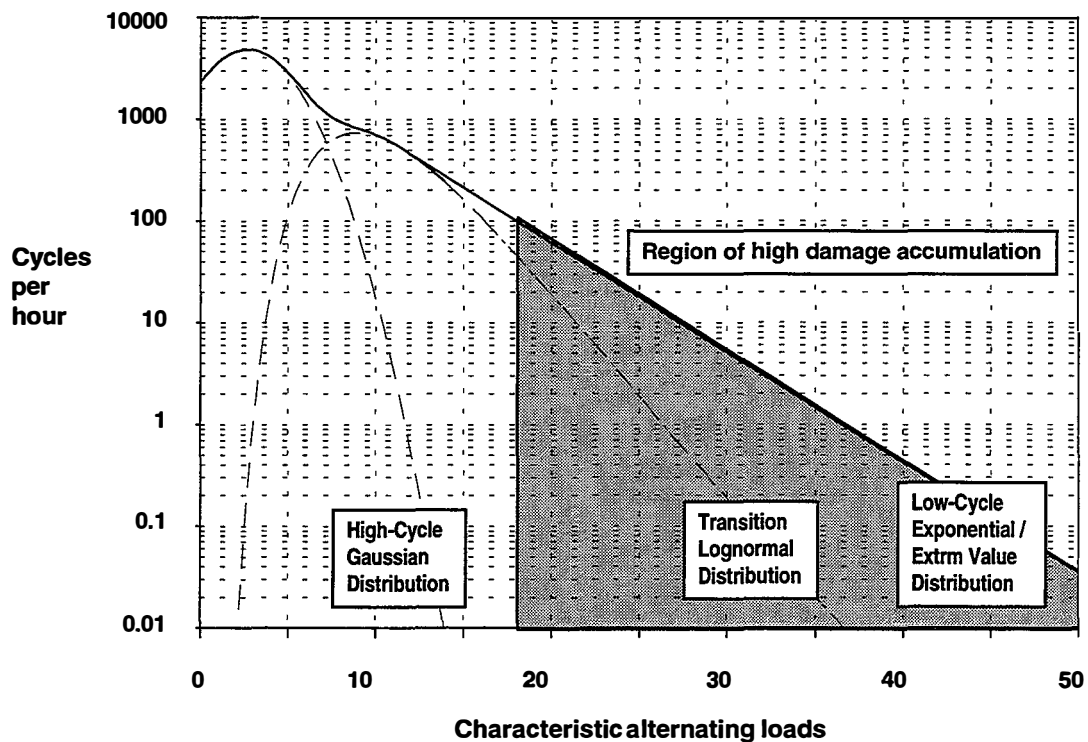


Figure 1. Schematic of Loading-Cycle Ranges and Mixed-Distribution Model.

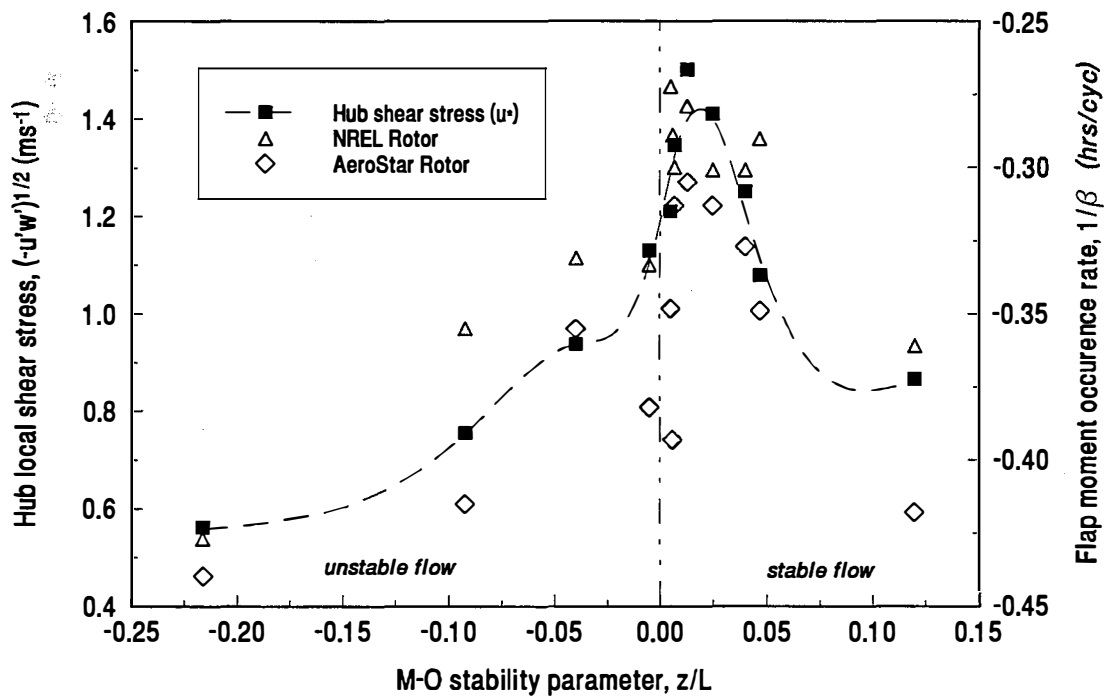


Figure 2. Variation of hub-level shear stress and exponential distribution shape parameter,  $\beta_1$ , for blade flapwise bending moment versus Monin-Obukhov (M-O) stability parameter,  $z/L$ .

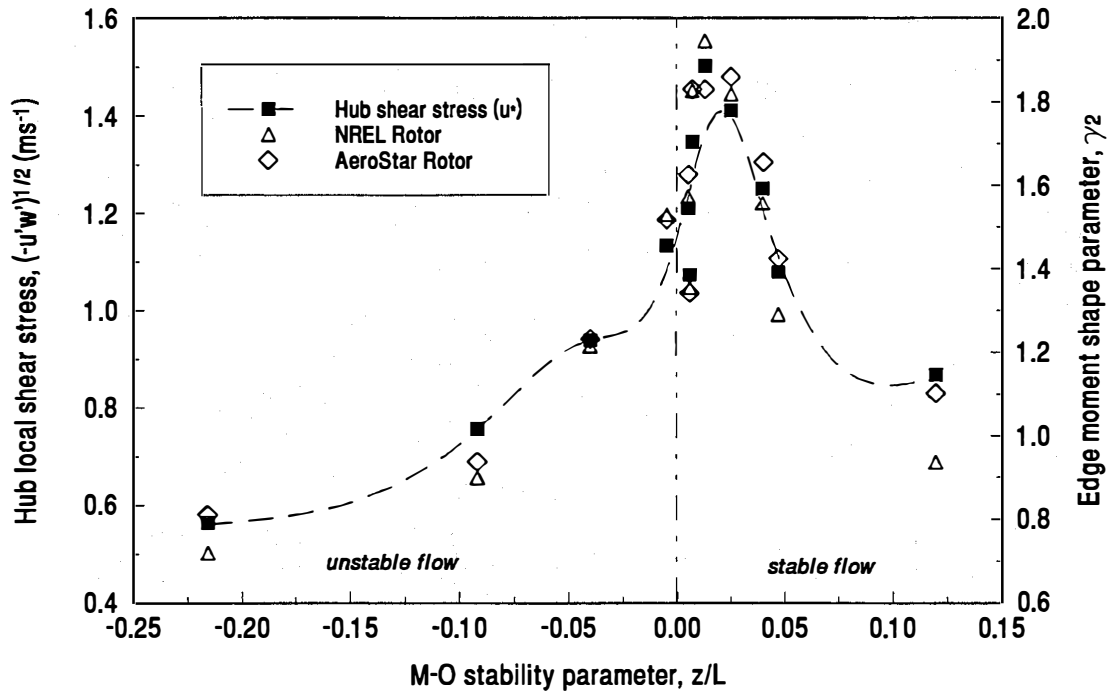


Figure 3. Variation of hub-level shear-stress and extreme-value distribution shape parameter,  $\gamma_2$ , for blade edgewise bending moment versus M-O stability parameter,  $z/L$ .

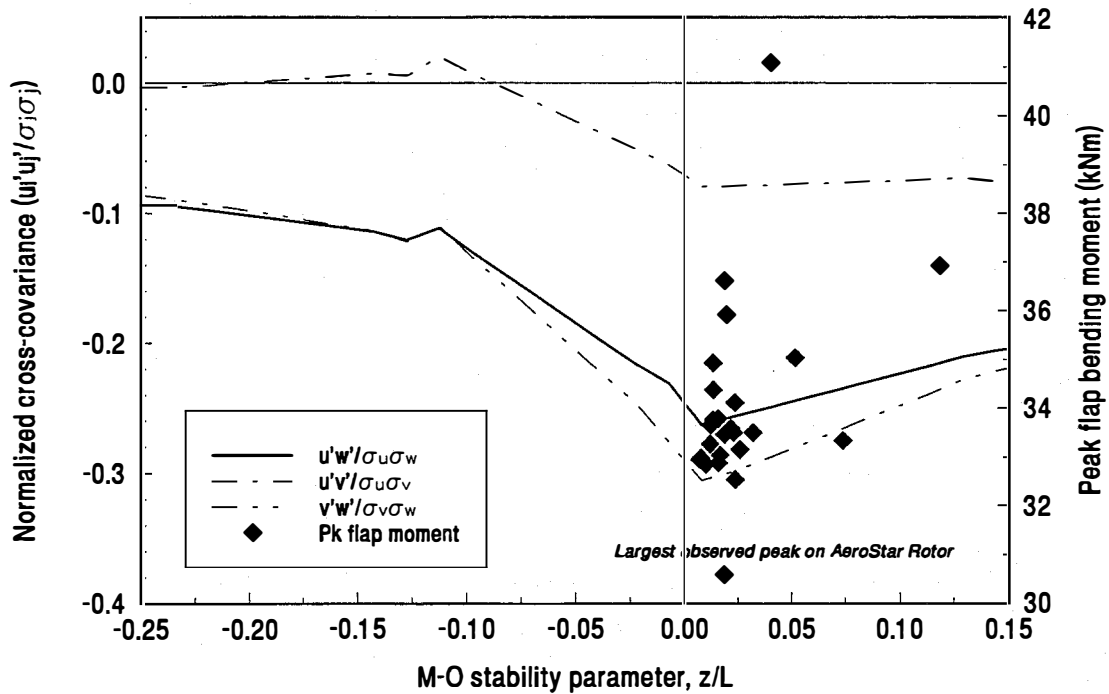


Figure 4. Wind-component normalized covariance versus M-O stability parameter,  $z/L$ . The peak flapwise loads for the 25 largest events are also shown.

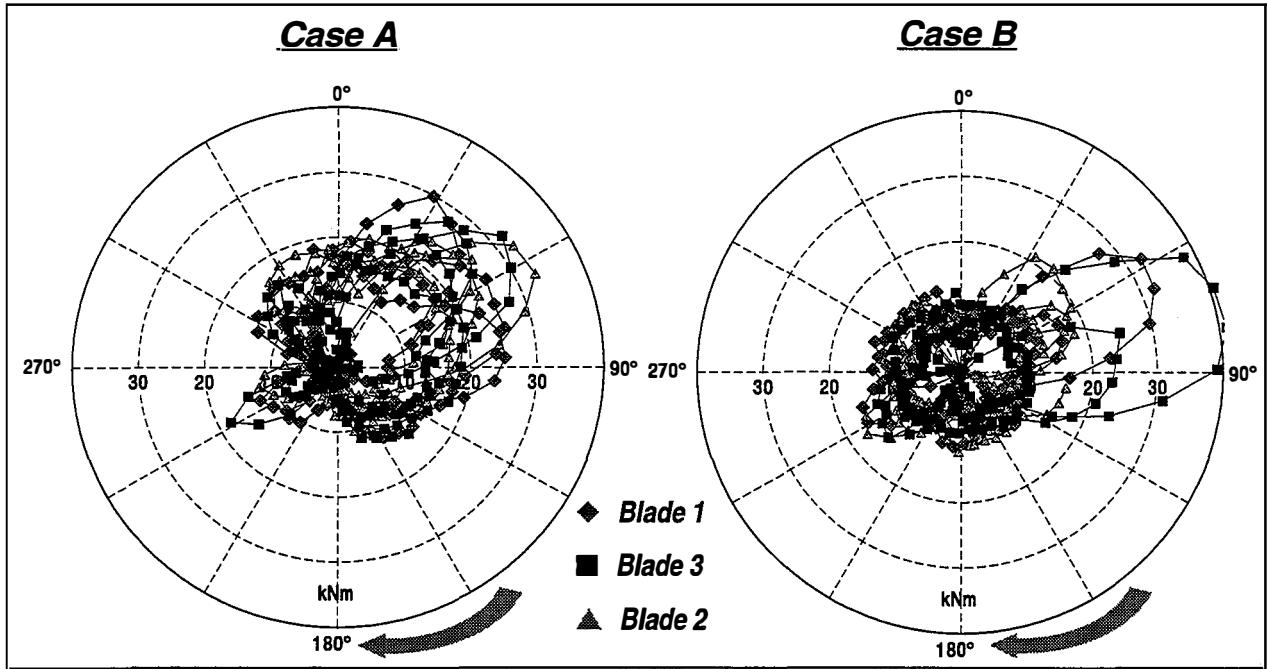


Figure 5. Azimuthal positions of peak flap loads observed on Micon 65 with NREL rotor. Case A is for less-stable flow ( $z/L = +0.007$ ) and Case B is for more-stable flow ( $z/L = +0.041$ ).

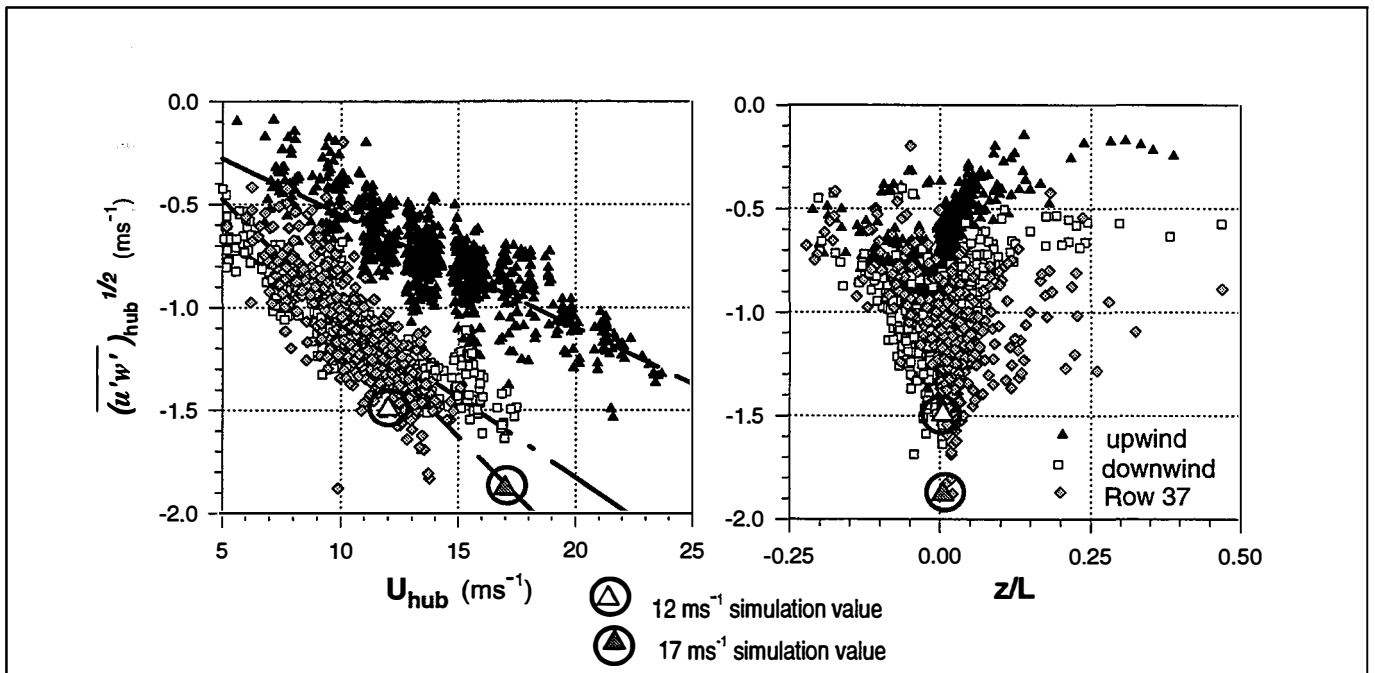


Figure 6. Variation of hub-height shearing stress with mean wind speed and stability parameter,  $z/L$ , for upwind, downwind, and at Row 37 in the San Gorgonio wind farm. Values calculated for the two turbulence simulations are also shown.

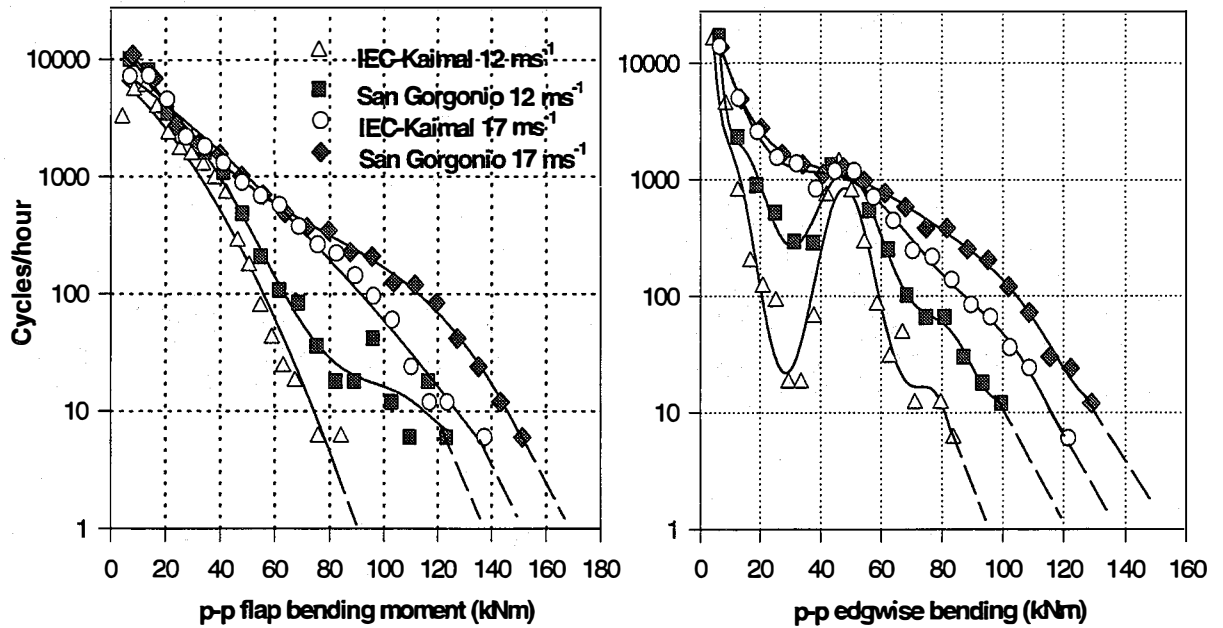


Figure 7. Predicted alternating flap- and edgewise load spectra for the four simulated turbulent inflow conditions.

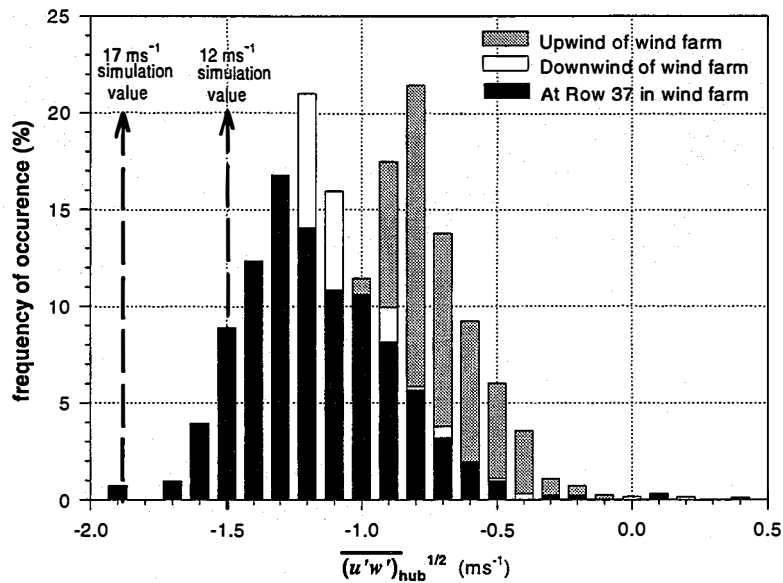


Figure 8. Observed mean  $u'w'$  mean shear-stress distribution for upwind, downwind, and Row 37.

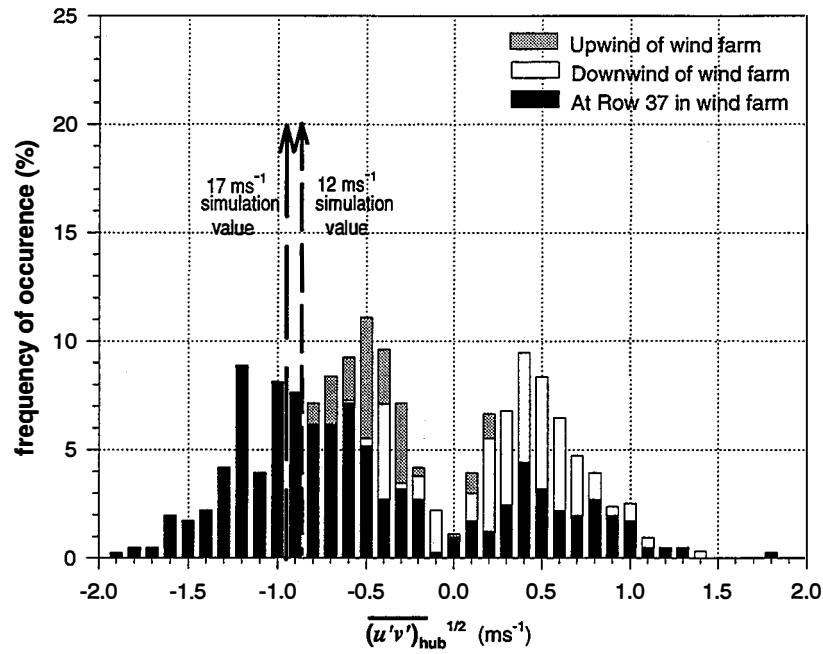


Figure 9. Observed mean  $u'v'$  mean shear stress distribution for upwind, downwind, and Row 37.

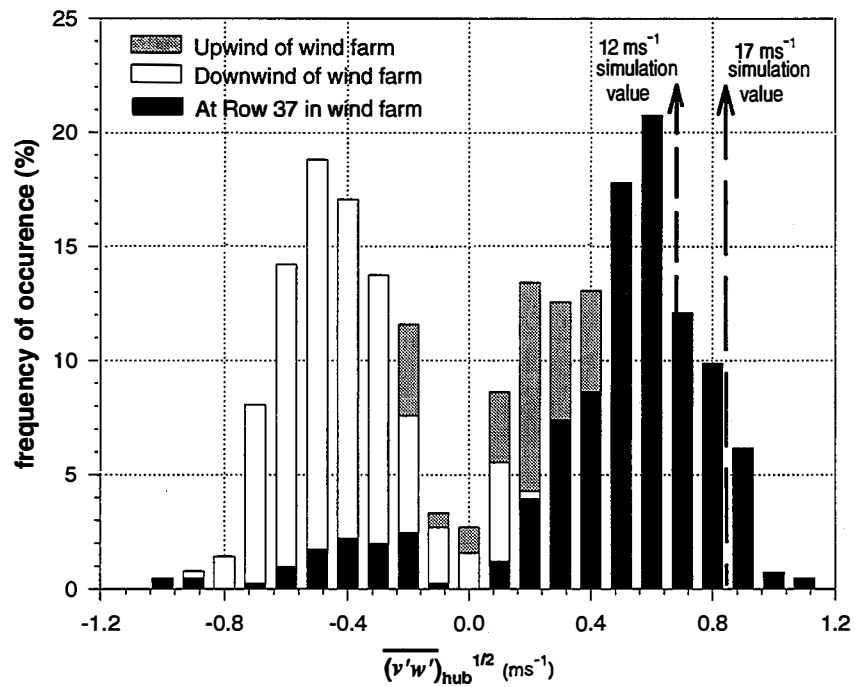


Figure 10. Observed mean  $v'w'$  mean shear stress distribution for upwind, downwind, and Row 37.

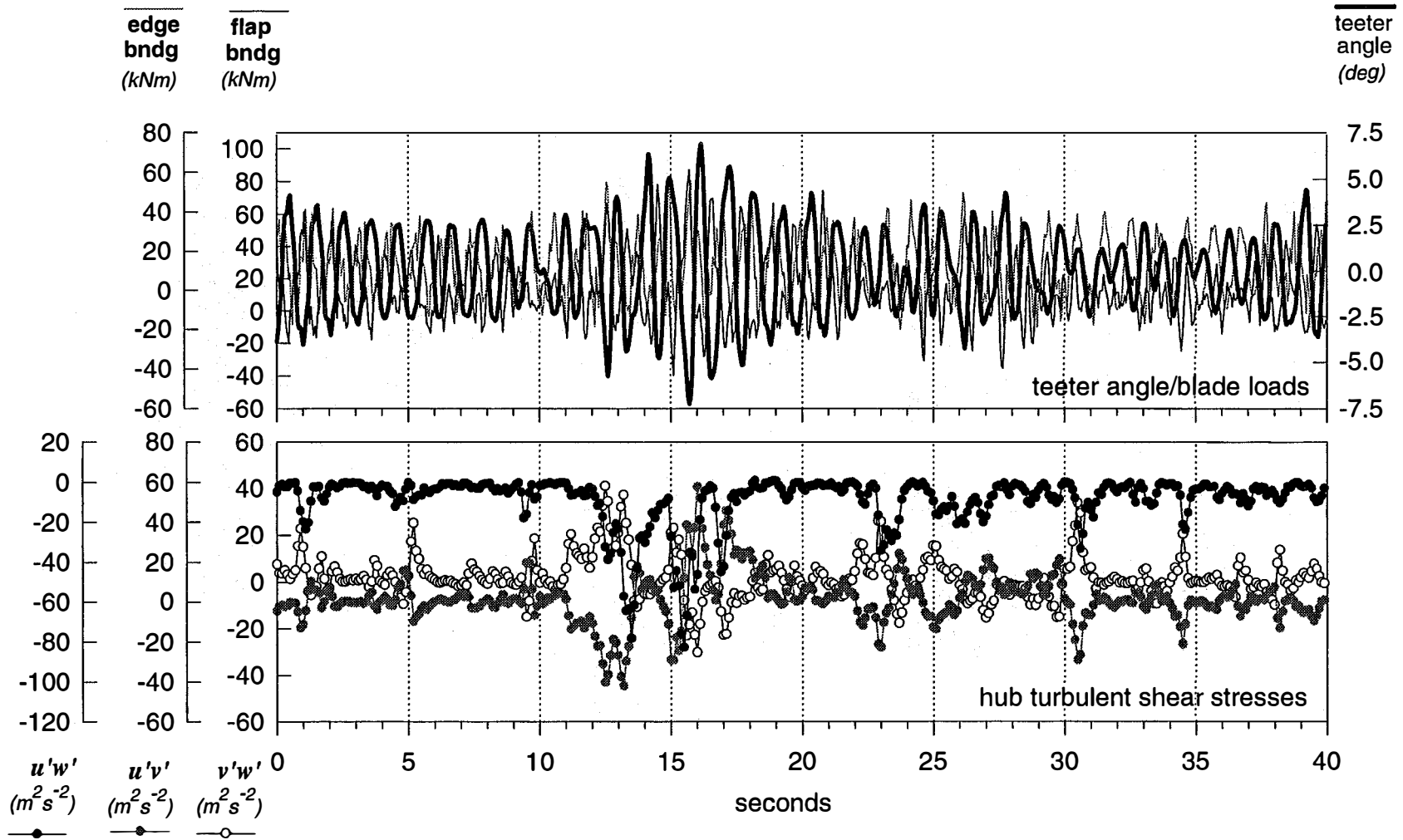


Figure 11. Simulated coherent blade loading example derived from  $17 \text{ ms}^{-1}$  San Gorgonio wind-farm turbulence model. Bending units are in kilonewton-meters (kNm).